DARK CURRENT STUDIES IN THE CLARA FRONT-END INJECTOR

F. Jackson, I. R. Gessey, J.W. McKenzie, B. L. Militsyn, P. Tipping
Cockcroft Institute, Warrington, Cheshire; STFC/DL/ASTeC, Daresbury, Warrington, Cheshire,UK

Abstract

At STFC Daresbury Laboratory a new facility CLARA (Compact Linear Accelerator for Research and Applications) is being designed and constructed. The principal aim of CLARA is advanced Free Electron Laser research. Halo and dark current in CLARA is a concern for damage to the undulator, and other applications of the machine. Recently the front end (gun, diagnostics, first linac) of CLARA has been installed including some collimation to mitigate halo effects. Beam halo may arise from gun field emission or due to beam dynamics in the early stages of acceleration, which may achieve the same energy as the core beam and thus may be transported to the undulator. The code CST is used to study the gun field emission. The code ASTRA is used to study the transport of field emission through the front end, including the effectiveness of collimators. Machine measurements of dark current are compared against these simulations.

INTRODUCTION

Many Free Electron Laser (FEL) accelerators, particularly those of high average power, use collimation to reduce potential damage to undulator magnets from beam halo particles [1-3]. Halo particles may arise from many sources, with field emission (dark current) from the electron gun particularly of interest since it may reach the same energy as the core beam and thus be more likely to reach the undulator.

CLARA [4] is a facility under design and construction at Daresbury Laboratory, UK, with the goal of advanced FEL research. CLARA encompasses VELA (Versatile Electron Linear Accelerator) which is a facility to provide a separate electron beam for other accelerator research and exploitation. Although in many of its design operational modes, including 100 Hz, the CLARA beam power is relatively low (< 10 W average), prolonged exposure of the undulator magnets to halo particles could lead to their demagnetisation. In addition, existing experience with operation of VELA indicates other undesirable effects of beam halo, particularly dark current, in non-FEL applications. Some measurements of dark current have been made on VELA [5].

Detailed simulation of dark current is presented here, using the codes CST [6] and ASTRA [7] in the VELA/CLARA front end injector which has recently been installed at Daresbury, see Fig. 1. Previously, a 2.5 cell S-band RF electron gun was operated on the VELA beam line [5]. First commissioning of the CLARA beam line includes using this gun (with new cathode) to inject into 2m long S-band linac1 .

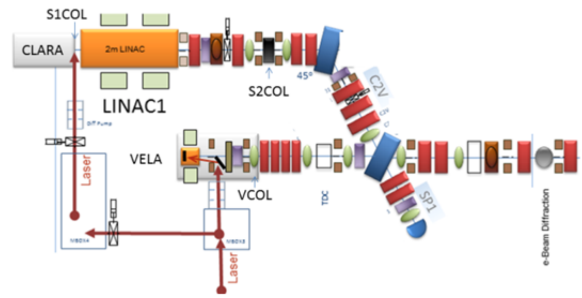

Figure 1: CLARA (top) and VELA (bottom) front end injector. Positions of plate collimators VCOL and S1COL are indicated, as is the post-linac collimator S2COL.

In this study we seek to simulate the production and transport of dark current from the 2.5 cell gun in both the VELA and CLARA lines and compare with experimental measurements. The production of dark current from similar guns is an active area of accelerator research [8] [9].

SIMULATION DETAILS

For simulation of creation and initial transport of dark current particles from gun field emission we use the code CST, a fully 3D tool. The electric field in the gun is modelled by the detailed geometry of the cavity using a finite element eigenmode EM solver, and the flux of dark current from various interior gun surfaces, all copper (see Fig. 2.), is simulated with the Fowler Nordheim empirical model [10] of field emission. The copper backplate of the gun serves as the photocathode. The 3D solenoid field was simulated from the original OPERA design and imported into CST, and includes a bucking coil to ensure the magnetic field is zero on the photocathode. Using nominal parameters (gun peak field of 70 MV/m and solenoid peak field of around 0.15 T) it was found that the only dark current which escapes the gun originates from the surface of the backplate.

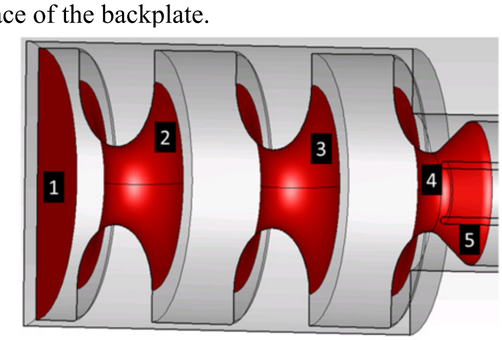

Figure 2: Emission points included in the simulation. Backplate (1), irises (2)-(5).

The field emission particle-in-cell solver applied to the surface of the backplate uses 4000 emission points in a regular grid and the number of emission points was chosen such that the basic phase space distributions of the

ISBN 978-3-95450-182-3

dark current particles converged. The Fowler-Nordheim scaling parameters were chosen such that the total amount of charge escaping the gun is a realistic value, at which space charge effects in the dark current are negligible, and based on previous observations of < 1 nC per RF pulse of 3 µs. In CST the charge of each macro particle is determined internally but the minimum macro charge was set to be that of a single electron. The dark current was transported to around 50 cm from the cathode which is outside the influence of the gun or solenoid fields.

For further transport of the dark current through VELA/CLARA, the macro charge 6D phase space output was transferred to ASTRA. The time values of the CST particles are converted to longitudinal position for input to ASTRA using the speed of each macroparticle (some are not ultra-relativisitic). The particles are then tracked solely in ASTRA in which the apertures, quadrupoles, and linac1 are modelled, and space charge is disabled since it has negligible effect.

Collimators exist as plate apertures on VELA and CLARA in diagnostic stages, and a thick collimator exists downstream of linac1 (see Fig. 1.) . The beampipe apertures include small apertures at the photoinjector laser light box, linac1 entrance, and cavity BPM in VELA (a diagnostics development project).

2.5 CELL GUN BASIC FEATURES OF DARK CURRENT

As described above, a gun gradient (peak field) of 70 MV/m was simulated which was the typical gradient used in VELA. Solenoid values of 3 different strengths were used, with the median value being close to the value which was typically used in beam transport. In every case the bucking solenoid was always set such that the B-field on the cathode was zero.

It was observed that the dark current formed distinct but similar longitudinal ‘bunches’ corresponding to RF cycles which were largely independent and that the inclusion of secondaries in the simulations did not alter this observation. The following plots thus are for one ‘bunch’ only.

The transverse distributions are cylindrically symmetric in x/y. The 2-D x/y distribution is shown in Fig. 3 and indicates the ‘twisting’ action of the solenoid; the camera image is from a screen ~ 50 cm further downstream than the simulation output. The filaments are observable in the simulations because the emission points on the backplate are discretely spaced on a regular grid; the observed pattern on the screen is similar thus suggesting discretely spaced field emitters on the back plate. The filaments then consist of varied energies as observed in [9]. The x–phase space distrubtion and x-momentum projection are shown in Fig. 4. This shows that particles with small transverse offsets and small transverse momentum are most likely to escape the gun and strong solenoids leads to overfocussing of the dark current. The correlation in the x, p_x distribution indicates the focussing effect of the gun/solenoid.

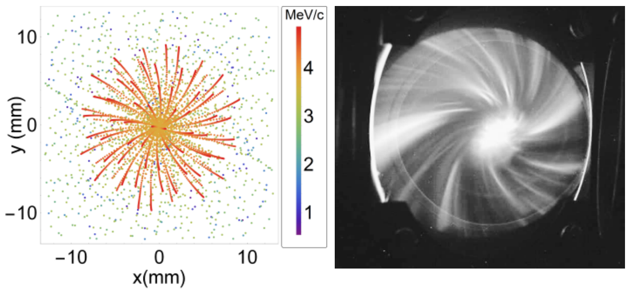

Figure 3: (Left) x/y distribution of simulated dark current macro particle distribution at gun exit (solenoid = 0.18 T) and (right) for comparison observed dark current on the first beamline screen in VELA. The colour scale is particle momentum.

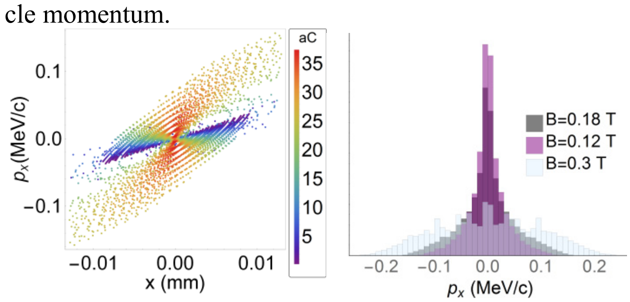

Figure 4: (Left) dark current space transverse phase space distribution (solenoid = 0.18 T) and (right) projection for 3 solenoid values. The colour scale on the 2-D plot is the macro particle charge in attoCoulombs.

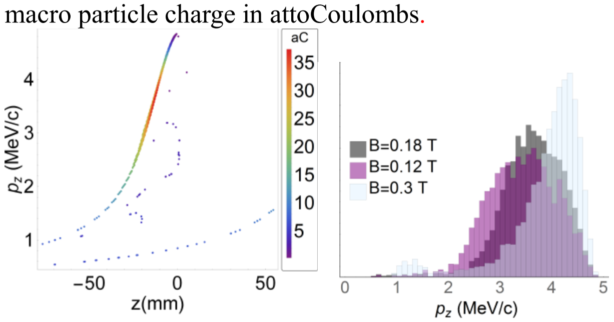

Figure 5: (Left) dark current longitudinal phase space distribution (solenoid = 0.18 T) and momentum projection (right) projection. See Fig. 5 for description of colours.

The longitudinal phase space of the dark current is shown in Fig. 5 and indicates the expected strong correlation in momentum and longitudinal position of the particles. The momentum projection indicates that the solenoid significantly affects the momentum distribution of the escaping dark current particles, with stronger solenoid leading to a larger proportion of higher momentum particles surviving.

A more detailed examination of the relative charge extracted from the gun vs solenoid strength was performed with more solenoid values and is shown in Fig. 6. For each main solenoid strength the bucking coil was set to cancel the field on cathode. This can be compared to data taken in 2014 and shows similarity, with dark current largest at intermediate solenoid values.

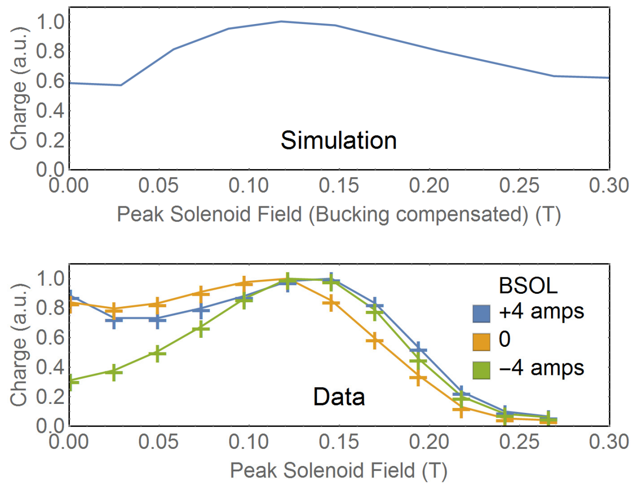

Figure 6: Total dark current charge escaping the gun/solenoid field (top simulated, bottom measured), vs peak solenoid field value. The colours in the bottom plot denote different bucking solenoid values.

DARK CURRENT TRANSPORT IN VELA

The efficiency of transport of dark current through the VELA line was simulated (see Fig. 7). In 2014/15 VELA operation, dark current was transported through the VELA line and measured on a wall current monitor (WCM) close to the gun and a faraday cup (FCUP) ~ 10 m downstream. The transport of the dark current to the FCUP was maximised with quadrupole focussing in an ad-hoc manner. The measured efficiency of dark current transport from WCM to the FCUP location was found to be ~ 2 %. Using the same gun/solenoid/quadrupole parameters as in the experiment, the transport of the dark current was simulated in CST/ASTRA (see Fig. 7). The ratio of simulated dark current surviving at the FCUP to that at the WCM is 8%. The plate collimator VCOL at 1 m from the gun has a significant impact on the dark current transport. It can be seen that the collimator's effect is relatively small at large z distance.

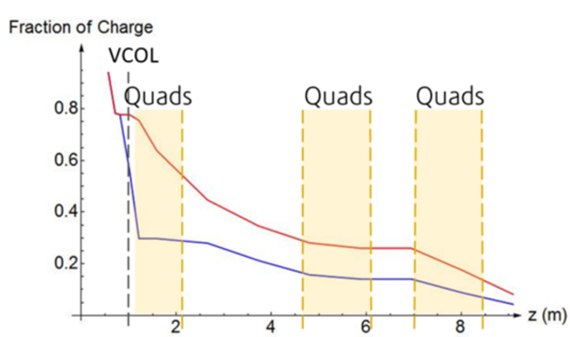

Figure 7: Dark current charge (vertical) surviving along VELA beamline distance (horizontal), for no collimator (red) and 6.3 mm diameter collimator at 1 m (blue).

DARK CURRENT TRANSPORT THROUGH CLARA FRONT END

Simulated transport of the dark current through the CLARA front end including linac1 and the post-linac collimator was also performed. The linac was set to gradient 21 MV/m, on crest, and the magnets set to the design for one of the main modes of CLARA FEL operation. The surviving dark current is shown in Fig. 8, indicating a significant loss of dark current at the linac entrance.

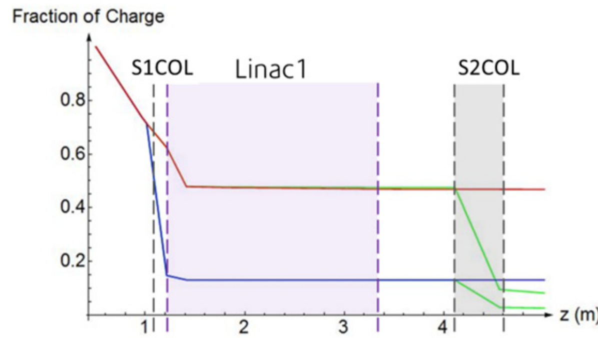

Figure 8: Dark current surviving in CLARA front end beamline. Linac 1 entrance is at 1.2 m, exit at 3.4 m. Collimators exist at z = 1.1 m and 4 m. Results are shown for no collimation (red), first collimator closed (blue), second collimator closed (green).

With no collimators in place, nearly 50 % of the initial dark current is transported to the exit of the CLARA front end. With tightest collimators in place, (4 mm diameter at entrance to linac-1, and 3 mm diameter S2COL), 2.5% survives. The linac phase set to -20° does not affect these observations; and while there is significant loss at the linac entrance, the rest of the linac sees very little loss.

CONCLUSIONS

Dark current from the 2.5 cell gun used on VELA and CLARA has been simulated, and some agreement is observed to measured quantities. While significant loss of dark current on the beampipe is observed in both the CLARA front end and VELA, collimators are observed in simulations to add significant power to mitigate halo transport through the machine.

These preliminary simulations form a useful tool to understand future dark current measurements on VELA/CLARA. No imperfections are included; significant sources of imperfection include the non-uniformity of field emission from the cathode surface, and non-perfect solenoid/RF fields.

ACKNOWLEDGEMENTS

We thank L. Cowie, P. Goudket, B. Shepherd for assistance with the simulation of RF and magnetic fields.

REFERENCES

[1] S. Di Mitri *et al.*, "Influence of longitudinally tapered collimators on a high brightness electron beam", Phys. Rev. ST Accel. Beams, vol. 15, p 061001 (2012).

[2] F. Jackson *et al.*, "Collimation System Design and Performance for the SwissFEL", *Proc. IPAC '12*, New Orleans, USA, 2012, paper TUPPP067.

[3] L. Froelich, "Machine Protection for FLASH and the European XFEL", Ph.D. thesis, Phys. Dept., Hamburg University, Germany, (2009).

ISBN 978-3-95450-182-3

[4] J A Clarke *et al.*, "CLARA conceptual design report", *Journal of Instrumentation*, vol. 9., 5, T05001, (2014).

[5] D J Scott *et al.*, "VELA Machine Development and Beam Characterisation", *Proc. IPAC '15*, Richmond, USA, 2015, paper TUPJE056.

[6] CST Studio 2015, Computer Simulation Technology AG, Darmstadt, Germany, `http://www.cst.com`

[7] K. Floettmann, A Space Charge Tracking Algorithm ASTRA, `http://www.desy.de/~mpyflo/`

[8] H. Chen *et al*., "Surface Emission Studies in a High-Field RF Gun based on Measurements of Field Emission and Schottky-Enabled Photoemission", *Phys. Rev. Lett*. vol 109, p. 204802, (2012).

[9] J. H. Shao *et al*., "Dark Current Imaging Experiment in a L-Band RF Gun", Proc IPAC '15, Richmond, USA, paper WEPMN015.

[10] R. H. Fowler and L. Nordheim, "Electron emission in intense electric fields", in *Proc. Roy. Soc*. (London), vol. 119, pp. 173–181, 1928.